

# Singularities in Electro- and Magnetostatics, and Their Efficient Resolution by *hp*-FEM

Pavel Šolín<sup>1</sup>, Martin Zítka

Department of Mathematical Sciences, University of Texas at El Paso  
Institute of Electrical Engineering, Academy of Sciences of the Czech Republic

Karel Segeth<sup>2</sup>

Mathematical Institute, Academy of Sciences of the Czech Republic  
Faculty of Education, Technical University of Liberec

## Abstract

In this paper we review the derivation of the partial differential equations describing electro- and magnetostatics from the Maxwell's equations of electromagnetics, explain the major difficulties related to their efficient and accurate numerical solution, and give an overview of basic ideas of the *hp*-FEM. An example electrostatics problem is used to illustrate the superiority of the *hp*-FEM over the standard FEM in terms of the number of degrees of freedom and CPU time.

**Keywords:** electrostatics, magnetostatics, potential equation, singular solution, *hp*-FEM

## 1 Introduction

The problems of electro- and magnetostatics are described in terms of rather simple elliptic partial differential equations that are obtained from the Maxwell's equations of electromagnetics by introducing suitable scalar potentials and applying appropriate constitutive relations. Since this procedure does not seem to be very familiar to the mathematical audience, we find useful to review it in Section 2 of this paper. The mathematical theory of elliptic equations has been well-established long time ago, and elliptic problems are known to be well-posed

---

<sup>1</sup>P. Šolín and M. Zítka acknowledge the financial support of the Czech Science Foundation under the Project No. 102/05/0629.

<sup>2</sup>K. Segeth was supported by the Czech Science Foundation under Project No. 201/04/1503 and by the Academy of Sciences of the Czech Republic Institutional Research Plan AV0Z10190503.

and to have unique solutions under suitable assumptions on the coefficients and data. The numerical solution of electro- and magnetostatics problems generally is considered to be a simple routine task. It is one of the goals of this paper to point out that this is not completely true. The major challenges related to the numerical solution of magneto- and electrostatics problems are discussed in Section 3.

In the recent years we witness a rapidly increasing popularity of the *hp*-FEM. This version of the finite element method varies both the size and polynomial degree of the elements in order to optimize the accuracy and efficiency of the method. The exponential convergence of the *hp*-FEM for elliptic problems was discovered by Babuška et al (see [1] – [4]). Because of its unconditional exponential convergence, the *hp*-FEM is among the best known numerical schemes for elliptic problems. The basic ideas of the *hp*-FEM are summarized in Section 4. A numerical example comparing the performances of the standard piecewise-linear FEM and the *hp*-FEM is presented in Section 5.

## 2 Equations of Electro- and Magnetostatics

The Maxwell's equations consist of the *Ampère's law*, *Faraday's law* of induction, and *Gauss' laws* for electricity and magnetism. Consider a planar simply-connected area  $\mathcal{A}$  whose boundary  $\mathcal{C}$  is a closed smooth curve. The **Ampère's law**,

$$\int_{\mathcal{C}} \mathbf{H} \cdot d\mathbf{C} = I + \frac{d\Psi}{dt}, \quad (2.1)$$

postulates that the line integral of the tangential component of the magnetic field strength  $\mathbf{H}$  along  $\mathcal{C}$  is proportional to the total current passing through the area  $\mathcal{A}$  in the normal direction. This current is given by the sum of the *conductive current*  $I$  and *displacement current*  $d\Psi/dt$ . The conductive current  $I$  is a scalar quantity defined by

$$I = \int_{\mathcal{A}} \mathbf{J} \cdot \boldsymbol{\nu} dS,$$

where  $\mathbf{J}$  stands for the vector-valued *density of conductive currents*. The *dielectric flux*  $\Psi$  is defined by

$$\Psi = \int_{\mathcal{A}} \mathbf{D} \cdot \boldsymbol{\nu} \, dS,$$

where  $\mathbf{D}$  is the *electric flux density* and the symbol  $\boldsymbol{\nu}$  stands for the unit normal vector to  $\mathcal{A}$ , oriented positively with respect to the orientation of the curve  $\mathcal{C}$  (right-hand rule). The **Faraday's law of induction**,

$$\int_{\mathcal{C}} \mathbf{E} \cdot d\mathbf{C} = -\frac{d\Phi}{dt}, \quad (2.2)$$

represents an analogous rule for the electric field strength  $\mathbf{E}$ : the line integral of the tangential component of the electric field  $\mathbf{E}$  along any closed smooth planar loop  $\mathcal{C}$  is equal to the negative of the rate of temporal change of the *magnetic flux*  $\Phi$  through the corresponding area  $\mathcal{A}$  in the normal direction. The magnetic flux  $\Phi$  is defined by

$$\Phi = \int_{\mathcal{A}} \mathbf{B} \cdot \boldsymbol{\nu} \, dS.$$

The **Gauss' law for electricity**,

$$\Psi = \int_{\mathcal{S}} \mathbf{D} \cdot \boldsymbol{\nu} \, dS = Q, \quad (2.3)$$

says that the total dielectric flux  $\Psi$  out of any (simply-connected) volume  $\mathcal{V}$  with a sufficiently regular boundary  $\mathcal{S}$  is equal to the *total electric charge*  $Q$  contained in the volume  $\mathcal{V}$ . The total electric charge  $Q$  is defined by

$$Q = \int_{\mathcal{V}} \varrho \, d\mathbf{x},$$

where  $\varrho$  is the *electric charge density*. The symbol  $\boldsymbol{\nu}(\mathbf{x})$  stands for the outer normal vector to the surface  $\mathcal{S}$  at a point  $\mathbf{x} \in \mathcal{S}$ . Finally, the **Gauss' law for magnetism**,

$$\int_{\mathcal{S}} \mathbf{B} \cdot \boldsymbol{\nu} \, dS = 0, \quad (2.4)$$

postulates that the magnetic flux  $\Phi$  out of any volume  $\mathcal{V}$  with a boundary  $\mathcal{S}$  is zero, or, in other words, that the magnetic field is *divergence-free*.

The main advantage of the integral form of the Maxwell's equations is that it provides a good idea about the relations between the field sources and field quantities. Its computational application, however, is limited to rather simple problems, characterized by trivial geometries and linear material properties. For practical purposes it is desirable to transform the Maxwell's equations (2.1) – (2.4) into partial differential equations.

## 2.1 Maxwell's equations in differential form

The transformation of the equations (2.1) – (2.4) into partial differential equations is done by means of the Stokes' and Gauss' theorems of calculus. Let us begin with the Ampère's law: applying the Stokes' theorem to (2.1), we obtain

$$\int_{\mathcal{A}} (\nabla \times \mathbf{H}) \cdot \boldsymbol{\nu} \, dS = \int_{\mathcal{A}} \left( \mathbf{J} + \frac{\partial \mathbf{D}}{\partial t} \right) \cdot \boldsymbol{\nu} \, dS,$$

where  $\boldsymbol{\nu}$  is the outer normal unit vector to the area  $\mathcal{A}$ . From the fact that the area  $\mathcal{A}$  is arbitrary it follows that

$$\nabla \times \mathbf{H} = \mathbf{J} + \frac{\partial \mathbf{D}}{\partial t}. \quad (2.5)$$

Analogously the Faraday's law (2.2) leads to

$$\nabla \times \mathbf{E} = -\frac{\partial \mathbf{B}}{\partial t}, \quad (2.6)$$

and the Gauss' theorems (2.3) and (2.4) yield

$$\nabla \cdot \mathbf{D} = \rho \quad (2.7)$$

and

$$\nabla \cdot \mathbf{B} = 0. \quad (2.8)$$

Let us remark that the density of conductive currents  $\mathbf{J}$  may include both source currents and eddy currents. The above equations hold exactly only at

the regular points of the domain – on interfaces one has to impose special interface conditions (see, e.g., [5]).

Most methods of computational electromagnetics (both analytical and numerical) are based on the differential form of the Maxwell’s equations. The main advantage of the PDE model is its ability to include nonlinearities, anisotropy and other nontrivial aspects of field computations. Next let us formulate the constitutive relations between the field vectors and physical properties of involved media, that form an indivisible part of the electromagnetic field model.

## 2.2 Constitutive relations

The field vectors  $\mathbf{E}$ ,  $\mathbf{D}$ ,  $\mathbf{H}$  and  $\mathbf{B}$  are coupled with the media via the relations

$$\mathbf{D} = \epsilon \mathbf{E}, \quad (2.9)$$

$$\mathbf{B} = \mu \mathbf{H}, \quad (2.10)$$

$$\mathbf{J} = \gamma(\mathbf{E} + \mathbf{E}_v). \quad (2.11)$$

The symbols  $\epsilon$ ,  $\mu$  and  $\gamma$  denote the permittivity, magnetic permeability and electric conductivity, respectively. The material parameters are generally tensors that may either be constant, or functions of the position, direction, local values of the field, frequency or state variables (such as temperature or pressure). It is worth mentioning that in the special isotropic case when a tensor is diagonal with equal diagonal entries, the tensor-vector product can formally be replaced with the corresponding product of the vector and the diagonal entry. The quantity  $\mathbf{E}_v$  is the *intensity of applied forces* of, for instance, electrochemical, photovoltaic or thermoelectric origin. For further reference by

$$\mathbf{J}_a = \gamma \mathbf{E}_v$$

we denote the *applied current density*.

## 2.3 Scalar electric potential

It is well-known that every smooth vector field  $\mathbf{F}$  that is *irrotational*,

$$\nabla \times \mathbf{F} = \mathbf{0},$$

is the gradient of some scalar function  $\phi$ ,

$$\mathbf{F} = \nabla(\phi + C),$$

where  $C$  is an arbitrary constant. The function  $\phi$  is called the *potential* of  $\mathbf{F}$ .

In a stationary electric field ( $\mathbf{E} = \mathbf{E}(\mathbf{x})$  and  $\mathbf{D} = \mathbf{D}(\mathbf{x})$ ), the Faraday's law (2.6) reduces to

$$\nabla \times \mathbf{E} = \mathbf{0}, \tag{2.12}$$

which means that  $\mathbf{E}$  can be written in the form

$$\mathbf{E} = -\nabla(\varphi_e + C), \tag{2.13}$$

where  $\varphi_e$  is referred to as the *electric potential*. The minus sign in (2.13) is a standard convention, corresponding to the fact that (positive) work has to be done when a charge is moved toward a field produced by charge(s) of the same sign. The electric potential may be interpreted as the work needed to move a unit charge from one point of the electric field to another point. The constant  $C$  in the electric potential may be determined according to various criteria, for example, from the requirement  $\varphi_e(\mathbf{x}) \rightarrow 0$  as  $|\mathbf{x}| \rightarrow \infty$ .

It follows from (2.13) that for any two points  $A, B \in \mathbb{R}$  that are connected through a smooth curve  $\mathcal{C} : (0, 1) \rightarrow \mathbb{R}$  it holds

$$\int_{\mathcal{C}} \mathbf{E} \cdot d\mathcal{C} = \int_0^1 \mathbf{E}(\mathcal{C}(s)) \cdot \mathcal{C}'(s) ds = - \int_0^1 \nabla \varphi_e(\mathcal{C}(s)) \cdot \mathcal{C}'(s) ds = \varphi_e(A) - \varphi_e(B). \tag{2.14}$$

The difference of the electric potentials at points  $A$  and  $B$  is called *voltage* and denoted by  $u_{AB}$ . If the loop  $\mathcal{C}$  is closed, it holds

$$\int_{\mathcal{C}} \mathbf{E} \cdot d\mathcal{C} = 0 \tag{2.15}$$

(fields with this property are called *conservative*).

Point sets with the same potential (curves in 2D and surfaces in 3D) are called *equipotentials*. In 2D an equipotential curve  $\mathcal{C} \subset \mathbb{R}^k$  starting from a point  $A \in \mathbb{R}^k$  can be constructed easily (numerically) using the relation

$$\varphi_e(\mathcal{C}(s)) = \text{const} \Leftrightarrow \nabla\varphi_e(\mathcal{C}(s)) \cdot \mathcal{C}'(s) = 0 \Leftrightarrow \mathbf{E}(\mathcal{C}(s)) \cdot \mathcal{C}'(s) = 0 \quad (2.16)$$

(i.e.,  $\mathcal{C}$  is perpendicular to the field vector  $\mathbf{E}$  at every its point  $\mathcal{C}(s)$ ). The construction of equipotential surfaces in 3D is more difficult (and it may not a bad idea to leave this task to a visualization software).

Lines orthogonal to equipotentials are called *force lines*. Both in 2D and 3D they can be calculated easily via the relation

$$\nabla\varphi_e(\mathcal{C}(s)) \times \mathcal{C}'(s) = \mathbf{0} \Leftrightarrow \mathbf{E}(\mathcal{C}(s)) \times \mathcal{C}'(s) = \mathbf{0} \quad (2.17)$$

(i.e., the field vector  $\mathbf{E}$  is tangential to  $\mathcal{C}$  at every its point  $\mathcal{C}(s)$ ). The force lines connect different potential levels and, indeed, are not closed curves.

### Equation for $\varphi_e$

Putting together the Gauss' law for electricity (2.7), the constitutive relation (2.9) and the gradient expression (2.13) for the stationary electric field  $\mathbf{E}$ , we obtain a second-order elliptic partial differential equation

$$-\nabla \cdot (\epsilon \nabla \varphi_e) = \varrho. \quad (2.18)$$

This equation attains an especially simple form in the isotropic homogeneous case,

$$-\Delta \varphi_e = \frac{\varrho}{\epsilon}. \quad (2.19)$$

The equation (2.18) is considered in some bounded domain  $\Omega \subset \mathbb{R}$  and equipped with standard boundary conditions for second-order elliptic problems. The Dirichlet conditions represent a prescribed potential (voltage). Homogeneous

Neumann conditions are prescribed on the line/plane of symmetry in the case of symmetric problems, and nonhomogeneous Neumann conditions generally on the part of the boundary where the normal component  $\mathbf{E} \cdot \boldsymbol{\nu}$  of the electric field (which is equal to  $-\partial\varphi_e/\partial\nu$ ) is given. Homogeneous Neumann boundary condition may also be used, for example, far from the source where it is reasonable to assume that the field does not change anymore.

### Variational formulation and unique solvability

A variational formulation is obtained in the standard way. It is worth mentioning that it requires the components of  $\epsilon$  to be  $L^\infty$ -functions. Thus piecewise discontinuous coefficients corresponding to various materials are indeed possible, and the resulting potential still is a  $H^1$ -function. The existence and uniqueness of solution is a consequence of the Lax-Milgram lemma (under the assumption that the part  $\Gamma_D$  of  $\partial\Omega$  corresponding to the Dirichlet boundary conditions is not empty).

### Calculation of $\mathbf{E}$

After calculating the (continuous, elementwise-polynomial) distribution of the scalar electric potential  $\varphi_e$  in the computational domain  $\Omega_h$ , the electric field  $\mathbf{E}$  is obtained via the relation (2.13). It is interesting to observe that the tangential component of  $\mathbf{E} = -\nabla\varphi_e$  is continuous, i.e.,  $\mathbf{E}$  lies in the desired Hilbert space  $\mathbf{H}(\text{curl})$ .

## 2.4 Scalar magnetic potential

For a stationary electromagnetic field the Ampère's law (2.5) reduces to  $\nabla \times \mathbf{H} = \mathbf{J}$  ( $\partial\mathbf{D}/\partial t = \mathbf{0}$  is frequently assumed also for nonstationary fields with sufficiently slow time-variation). In domains where  $\mathbf{J} = \mathbf{0}$ , such as in the air and other insulators, the field  $\mathbf{H}$  is irrotational,

$$\nabla \times \mathbf{H} = \mathbf{0}. \tag{2.20}$$

Then one can introduce the *scalar magnetic potential*  $\varphi_m$  such that

$$\mathbf{H} = -\nabla(\varphi_m + C), \quad (2.21)$$

where  $C$  is an arbitrary constant. This constant can be defined, for example, by requesting  $\varphi_m = 0$  somewhere. The Gauss law for magnetism (2.8) together with the constitutive relation (2.10) yield a second-order elliptic equation

$$-\nabla \cdot (\mu \nabla \varphi_m) = 0,$$

which is analogous to the potential equation (2.18). The properties of the magnetic potential  $\varphi_m$  are analogous to the electric potential  $\varphi$ . It is worth mentioning that the above model does not cover a conductor-insulator interface. On such interfaces one has to consider suitable interface conditions. Equipotentials and force lines are defined in the same way as for the scalar electric potential  $\varphi$ .

### 3 Numerical Challenges

There are two basic challenges related to the numerical solution of the electro- and magnetostatics problems: re-entrant corners and material interfaces with large jumps of the material parameters. At the re-entrant corners, the gradient of the solution (i.e., the electric or the magnetic field) typically is singular, as shown in Fig. 1.

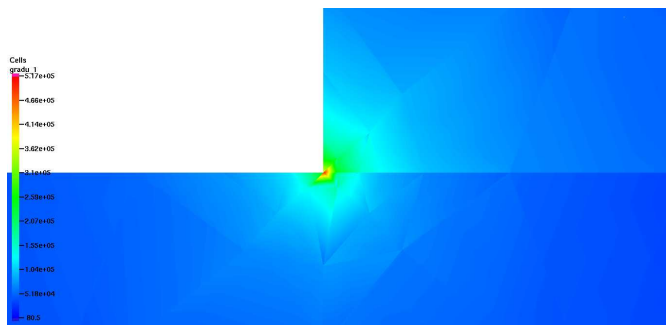


Figure 1: Singularity of  $|\mathbf{E}|$  at a re-entrant corner and discontinuity along a material interface (**zoom = 1000**).

An inaccurate resolution of the singularity induces a large contribution to the error,

$$\|e\|_{H^1(\Omega)} = \left( \int_{\Omega} e^2 + |\nabla e|^2 \, d\mathbf{x} \right)^{\frac{1}{2}}. \quad (3.22)$$

The singularities become the major source of error on higher levels of accuracy. Let us notice that usually they occur on a very small scale in space (such as, e.g.,  $10^{-3} - 10^{-6}$  of the characteristic length of the problem), and often they are not captured at all by simpler schemes such as FDM or lowest-order FEM without spatial refinement. The other major source of difficulty are the material interfaces. Here the jump in the material parameters, which can be in the range of several decimal orders, determines the gradient of the solution at the interface. These internal layers, too, usually are very local in space, but their inaccurate resolution leads to large contributions to the error (3.22).

## 4 Main Ideas of the *hp*-FEM

The *hp*-FEM is based on the fact that very smooth functions are optimally interpolated by means of high-degree polynomials in large elements, while low-degree polynomials in small elements optimally interpolate oscillatory and singular functions. This is illustrated in the following paragraph.

### 4.1 Motivation - an interpolation problem

By the Céa's lemma, the discretization error in  $V$ -elliptic problems is determined by the interpolation properties of the corresponding Galerkin subspace. In this paragraph we compare the quality of interpolation of very smooth functions by low-degree and higher-degree polynomials. Consider the function

$$g(x) = \cos\left(\frac{\pi x}{2}\right) \in V = H_0^1(-1, 1),$$

the subspace  $U_p = P_0^2(-1, 1) \subset V$  of quadratic polynomials with zeros at  $\pm 1$ , and the subspace  $U_h \subset V$  of continuous functions which also are zero at  $\pm 1$ , but piecewise-linear in the subintervals  $(-1, 0)$  and  $(0, 1)$ . These subspaces have

equal dimension,  $\dim(U_p) = \dim(U_h) = 1$ . We consider the inner product and norm

$$(\varphi, \psi)_V = \int_{-1}^1 \varphi'(x)\psi'(x) dx, \quad \|\varphi\|_V = \sqrt{(\varphi, \varphi)_V}$$

in the space  $V$ . By  $g_p$  and  $g_h$  denote the best interpolants of the function  $g$  in the subspaces  $U_p$  and  $U_h$ , respectively. Recall that when  $U$  is a closed subspace of a Hilbert space  $V$  and  $g \in V$ , then the best interpolant  $g_u \in U$  of  $g$  is a function in  $U$  which minimizes the norm  $\|g - g_u\|_V$ . The function  $g_u$  is the unique orthogonal projection of  $g$  onto  $U$ . Let us calculate the orthogonal projections now. The basis of the space  $V_h$  consists of the piecewise-linear function  $\hat{g}_h(x) = x + 1$  in  $(-1, 0]$ ,  $\hat{g}_h(x) = 1 - x$  in  $[0, 1)$ . Hence, the best interpolant of  $g$  in the space  $V_h$  has the form  $g_h = \alpha \hat{g}_h$ , where the real coefficient  $\alpha$  is determined from the orthogonality condition

$$(g - \alpha \hat{g}_h, \hat{g}_h)_V = 0.$$

It is easy to calculate that  $\alpha = 1$ . The functions  $g$  and  $g_h$  are shown in Fig. 2.

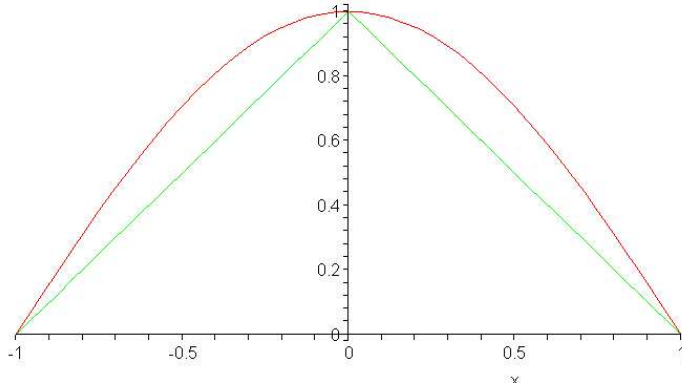


Figure 2: Best interpolant  $g_h \in V_h$  of the function  $g \in V$  in the space  $V_h$ . The interpolation error is  $\|g - g_p\|_V = 0.683667$ .

The function  $\hat{g}_p(x) = 1 - x^2$  is the basis of the space  $V_p$ , and the best interpolant of  $g$  in the space  $V_p$  has the form  $g_p = \beta \hat{g}_p$ , where the real coefficient

$\beta$  is determined from the orthogonality condition

$$(g - \beta \hat{g}_p, \hat{g}_p)_V = 0.$$

In this case  $\beta = 3/\pi$ . The functions  $g$  and  $g_p$  are shown in Fig. 3.

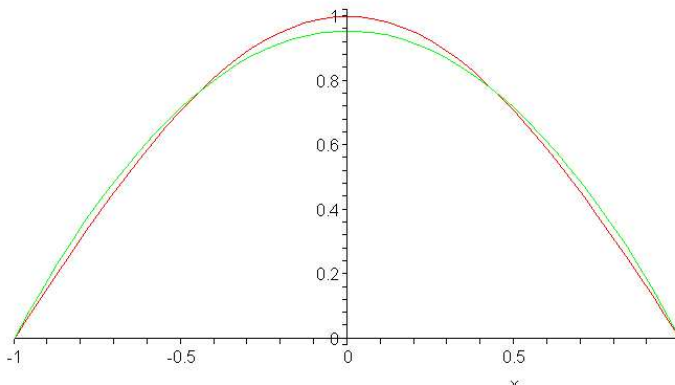


Figure 3: Best interpolant  $g_p \in V_p$  of the function  $g \in V$  in the space  $V_p$ . The interpolation error is  $\|g - g_p\|_V = 0.20275$ . Notice that this result is more than **three-times better** compared to the piecewise-linear case.

Vice-versa it holds that less regular functions with local changes or oscillations are interpolated better in piecewise low-order subspaces than by higher-order polynomials. Therefore the ultimately best Galerkin sequences  $V_1 \subset V_2 \dots \subset V$  are achieved via *hp-refinement* that combines *h*-refinements in subdomains of  $\Omega$  where the solution exhibits local or oscillatory behaviour, with *p*-refinement in subdomains of  $\Omega$  where the solution has a smooth, polynomial-like character.

## 4.2 Hierarchic shape functions

In order to combine elements with variable polynomial degrees, one needs a *hierarchic basis*. The hierarchic basis functions are usually constructed using a suitable set of hierarchic shape functions on a reference domain and suitable reference maps. On triangular elements, the hierarchic shape functions comprise

*vertex functions* that represent the solution at the vertices (Fig.4), *edge functions* that represent the solution on the edges (Fig. 5), and *bubble functions* that represent the solution in the element interior (Fig. 6). For more details we refer the reader to to [5, 8].

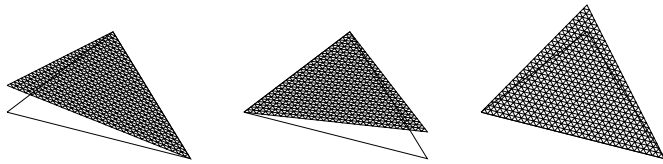


Figure 4: Vertex functions.

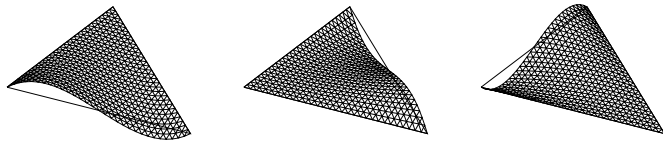


Figure 5: Cubic edge functions.

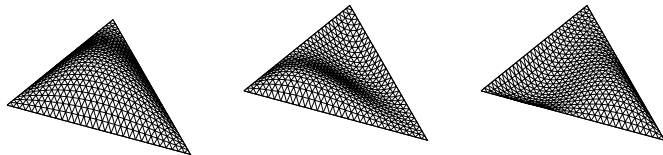


Figure 6: Cubic bubble function and fourth-order bubble functions.

### 4.3 $h$ -, $p$ - and $hp$ -adaptivity

The automatic adaptivity for  $hp$ -FEM is substantially different from the conventional spatial adaptivity ( $h$ -adaptivity) and the  $p$ -adaptivity (that only varies the polynomial degree of the elements). Namely, in these two last cases in principle a single value of an error estimate per element is enough to determine the new refined mesh. However, this is not sufficient for the  $hp$ -adaptivity, where

one needs to select the best option among several *competitive hp-refinements*. Thus, one needs the *shape* of the error, not only its magnitude. This is illustrated in Fig. 7.

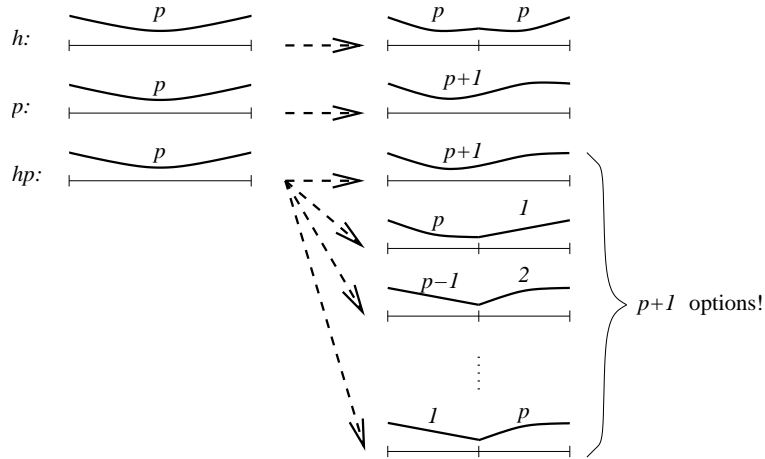


Figure 7:  $h$ -,  $p$ - and  $hp$ -refinement in 1D.

Let us remark that there are significantly more options for an  $hp$ -refinement in 2D and 3D. See, e.g., [6, 7, 8] for details.

#### 4.4 A-posteriori error estimation for $hp$ -adaptivity

As we saw above, one needs some information on the shape of the error (as a function) in order to select the optimal  $hp$ -refinement of an element. This information could in principle be extracted from estimates of the derivatives of the error. However, since this procedure is both highly nontrivial and equation-dependent, we prefer to approximate the error by means of a *reference solution*. The reference solution  $\varphi_{ref}$  is an approximation of the exact solution  $\varphi$  that is significantly more exact than the original approximate solution  $\varphi_{h,p}$ . Then the difference  $\varphi_{ref} - \varphi_{h,p}$  provides the desired estimate of the shape of the true error  $\varphi - \varphi_{h,p}$ . The reference solution can be obtained in various ways, for example using a globally  $hp$ -refined mesh and a two-grid solver (see, e.g., [6, 7, 8]). Another way is to compute the reference solution for every element separately

using a patch of elements. Such alternative offers excellent scalability of the error estimate on parallel computers. This is a work in progress.

## 5 Sphere-Cone problem

The advantage of the  $hp$ -FEM with respect to standard FEM is illustrated on an axisymmetric problem involving the electrostatic field between a charged sphere and a metallic cone:

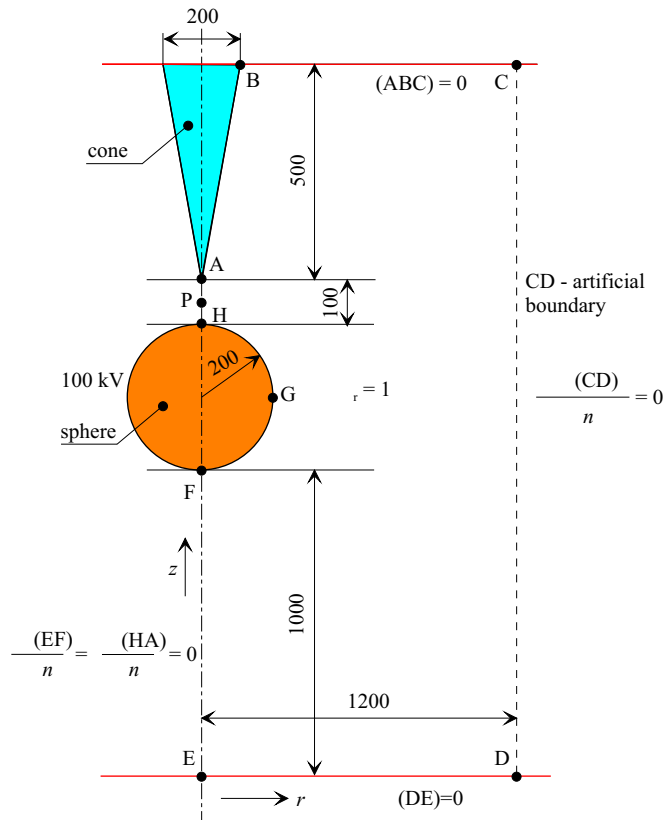


Figure 8: Computational domain (all measures are in millimeters). Electric potential of the sphere is  $\varphi = 100$  kV, the cone is grounded..

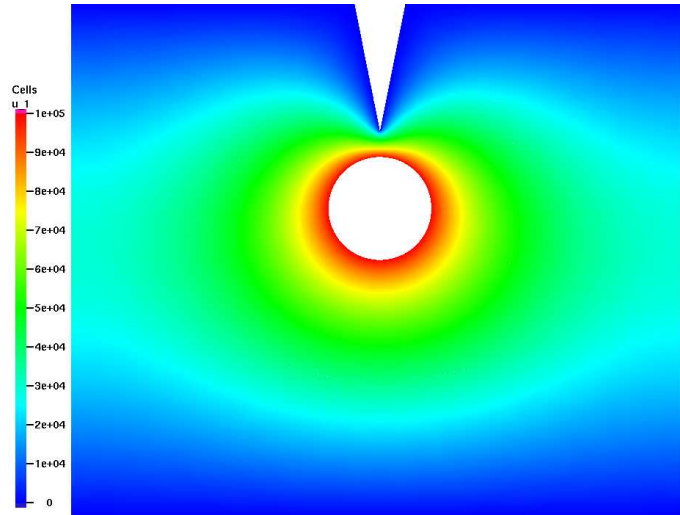


Figure 9: Solution of the cone-sphere problem (the electric potential  $\varphi$ ).

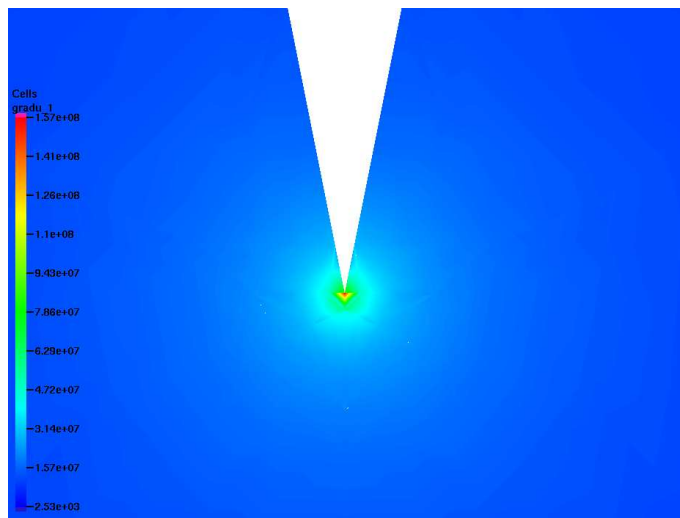


Figure 10: Detail of the singularity of  $|\mathbf{E}| = |-\nabla\varphi|$  at the tip of the cone (zoom = 100,000).

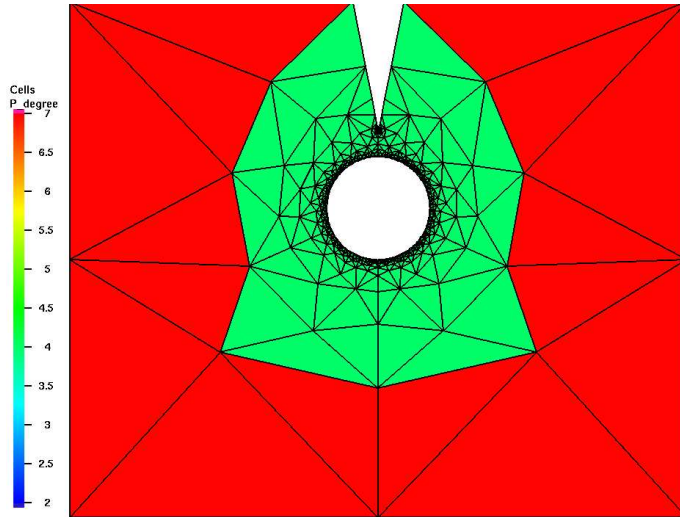


Figure 11: The  $hp$ -mesh – global view. Large seventh-order elements are used far from the singularity and small quadratic elements at the tip of the cone.

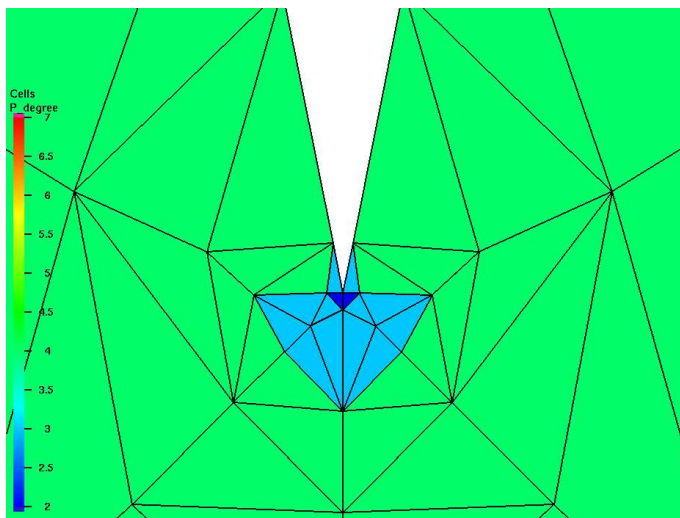


Figure 12: The  $hp$ -mesh – detail of the tip of the cone (zoom = 100,000).

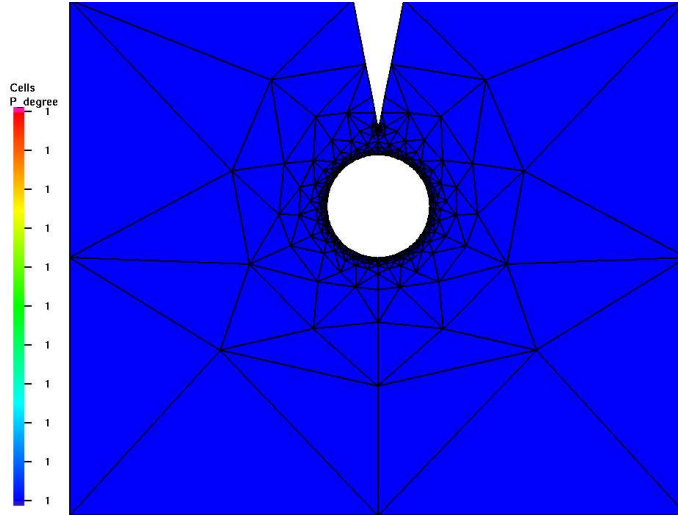


Figure 13: The piecewise-linear mesh. This mesh was uniformly refined for the computation in order to attain the prescribed accuracy (each edge was subdivided into 48).

The efficiency of the piecewise-linear FEM and the  $hp$ -FEM is compared in Table 1:

	linear elements	$hp$ -elements
DOF	488542	3317
Error	0.5858 %	0.2804 %
Iterations	859	44
CPU time	30 min.	10.53 sec.

## 6 Current research and outlook

Our current research is devoted to various theoretical and practical aspects of the  $hp$ -FEM. On the theoretical side we recently proved the discrete maximum principle for the  $hp$ -FEM in one spatial dimension [9], and it is our next goal to

extend this result to 2D and 3D. Further we investigate the possibility of using the energetic inner product associated with an elliptic problem to improve the conditioning properties of the hierarchic shape functions. We also investigate the possibility of replacing affine-equivalent elements with non-affine-equivalent elements with improved orthogonality properties in the mesh elements.

On the practical side we are developing object-oriented *hp*-FEM solvers ELSYS\_2D and ELSYS\_3D for two and three-dimensional problems. It is our goal to develop a robust modular object-oriented software package that will house various types of finite elements (continuous, edge, Taylor-Hood, etc.) based on a common platform that handles the *hp*-meshes, connectivity, *hp*-adaptivity, multigrid, etc. Currently, the 2D solver ELSYS\_2D is more mature, providing hierarchic continuous elements for second-order elliptic problems as well as hierarchic  $\mathbf{H}(\text{curl})$ -conforming edge elements for the Maxwell's equations, and various linear system solver packages (Trilinos, PETSc, UMFPACK). The first version of the 3D solver ELSYS\_3D, containing hierarchic continuous elements, is about to be finished and parallelized in Fall 2005. We further deal with numerous exciting open problems related to the optimization of automatic *hp*-adaptive algorithms and reference-solutions-based a-posteriori error estimators, parallelization of the codes, etc.

## References

- [1] I. Babuška, T. Strouboulis, K. Copps, *hp*-optimization of finite element approximations: Analysis of the optimal mesh sequences in one dimension, *Comput. Methods Appl. Mech. Engrg.* 150 (1997), 89–108.
- [2] I. Babuška, M. Suri, The optimal convergence rate of the *p*-version of the finite element method, *SIAM J. Numer. Anal.* 24 (1987), 750–776.
- [3] I. Babuška, M. Suri, The *p*- and *h-p* versions of the finite element method, *Comput. Methods Appl. Mech. Engrg.* 80 (1990), 5–26.
- [4] I. Babuška et al., Efficient preconditioning for the *p*-version finite element method in two dimensions, *SIAM J. Numer. Anal.* 28 (1991), 624–661.

- [5] P. Šolín: *Partial Differential Equations and the Finite Element Method*, J. Wiley & Sons, 2005.
- [6] P. Šolín, L. Demkowicz: Fully Automatic Goal-Oriented *hp*-Adaptivity for Elliptic Problems, *Comput. Methods Appl. Mech. Engrg.* 193 (2004), 449 - 468.
- [7] P. Šolín, L. Demkowicz: Automatic Goal-Oriented *hp*-Adaptivity Without Error Estimates, *Numerical Mathematics and Advanced Applications* 5, Berlin, Springer 2004, 775 - 785
- [8] P. Šolín, K. Segeth, I. Doležal: *Higher-Order Finite Element Methods*, Chapman & Hall/CRC Press, Boca Raton, 2003.
- [9] P. Šolín, T. Vejchodský: On the Discrete Maximum Principle for *hp*-FEM, submitted.
- [10] M. Zitka, K. Segeth, P. Šolín: Higher-order FEM for Systems of Nonlinear Parabolic PDEs with A-Posteriori Error Estimates. *Numerical Mathematics and Advanced Applications* 5, Berlin, Springer 2004, 854 - 863.
- [11] M. Zitka, P. Šolín, K. Segeth: PARSYS\_2D – a higher-order FE solver for systems of nonlinear elliptic and parabolic equations. In: *ECCOMAS 2004 CD ROM Vol. 2. (Proc. of Congress, Jyvaskyla 2004.)* Jyvaskyla, University of Jyvaskyla 2004, 15 pp.
- [12] M. Zitka, P. Šolín, K. Segeth: The *hp*-FEM Solver PARSYS\_2D and Applications in Electrostatics, *IGTE Conference*, September 13 - 15, 2004, Graz, Austria, Publishing House Graz University of Technology, pp. 51 - 56.